batteries

MDPI

Article

The Quantum-Inspired Evolutionary Algorithm in the Parametric Optimization of Lithium-Ion Battery Housing in the Multiple-Drop Test

Adam Rurański and Wacław Kuś *

Faculty of Mechanical Engineering, Silesian University of Technology, 44-100 Gliwice, Poland
* Correspondence: waclaw.kus@polsl.pl

Abstract: Recent developments in lithium-ion batteries have improved their capacity, which allows them to be used in more applications like power tools. However, they also carry higher risks, such as thermal runaway, which can happen if they are damaged. To make these batteries safer, it is important to improve the design of their housings subjected to multiple drops during their use. This article introduces a new method for optimizing the design of lithium-ion battery housings using a Quantum-Inspired Evolutionary Algorithm (QEA). Previously used mainly in theoretical settings, the authors have adapted QEA for practical engineering tasks. Multiple-drop test simulations were performed, and QEA was used to identify the best housing designs that minimize damage. To support this, a program was developed that automates all drop tests and rebuilds the model. The damage is obtained on the basis of the finite element method (FEM) analyses. The findings show that the algorithm successfully identified designs with the least damage during these tests. This research helps make battery housings safer and explores new uses for QEA in mechanical engineering.

Keywords: Quantum-Inspired Evolutionary Algorithm; optimization; multiple-drop test; FEM; Li-ion battery housing

Citation: Rurański, A.; Kuś, W. The Quantum-Inspired Evolutionary Algorithm in the Parametric Optimization of Lithium-Ion Battery Housing in the Multiple-Drop Test. *Batteries* **2024**, *10*, 308. https://doi.org/10.3390/batteries10090308

Academic Editor: Wilhelm Pfleging

Received: 19 June 2024
Revised: 27 August 2024
Accepted: 29 August 2024
Published: 31 August 2024

1. Introduction

The development of battery cells in the last few years has resulted in new chemistries, which caused a significant increase in electrical capacity. This has opened up new opportunities to implement batteries in applications where it was previously not possible due to their high mass, volume, or insufficient capacity. As a result, lithium-ion batteries started to be widely used in power tools, garden tools, and other common household devices. In 2009, W. Weyland predicted that li-ion cells would have a significant participation in the market, which can be confirmed by the present situation [1]. Recent papers also show that this trend will continue [2,3]. Li-ion batteries have many advantages but also provide additional challenges to solve. The high energy density also increases the potential risks associated with devices that use these batteries. Lithium-ion cells, when damaged, are sensitive to a phenomenon known as thermal runaway [4]. Thermal runaway can be initiated by mechanical, thermal, chemical, and electrical factors. The progression of this phenomenon is often comparable to an explosion [5]. A single cell is constructed from layers (anode and cathode), and when a short circuit occurs between these layers, the thermal runaway phenomenon is initiated. This phenomenon has catastrophic effects, similar to chain reaction, where surrounding cells can also experience the same phenomenon, and it becomes uncontrollable. Due to the growing demand for electrical tools and high potential risk involved, a greater focus is required on their safety.

From an electrical perspective, the Battery Management System ensures the safety of the battery by monitoring its voltage balance and other electrical parameters [6]. It can also shut the battery down when any electrical parameter reaches a dangerous level. However, from a mechanical perspective, once a Li-ion cell is damaged, there is no way to

stop the reaction. Although engineers try to find methods to simulate and limit the effects of thermal runaway when it occurs, it is still better to prevent the start of this phenomenon from initiating rather than to mitigate its effects [5,7].

The typical mechanical tests to which batteries are subjected focus on simulating conditions occurring during battery transportation [8–13]. These tests include vibration tests (both harmonic and random vibrations) and shock tests (acceleration or deceleration, e.g., 150 G). However, it is important to note that various mechanical events can also occur during normal everyday work with handheld power tools, such as drops or impacts. Among these, the drop test is crucial in relation to natural human awkwardness and accidents, where drop incidents can occur during the usage of a power tool and, e.g., battery replacement. Drop events can occur for the whole tool and only on the battery, which is presented in a simplified way in Figure 1.

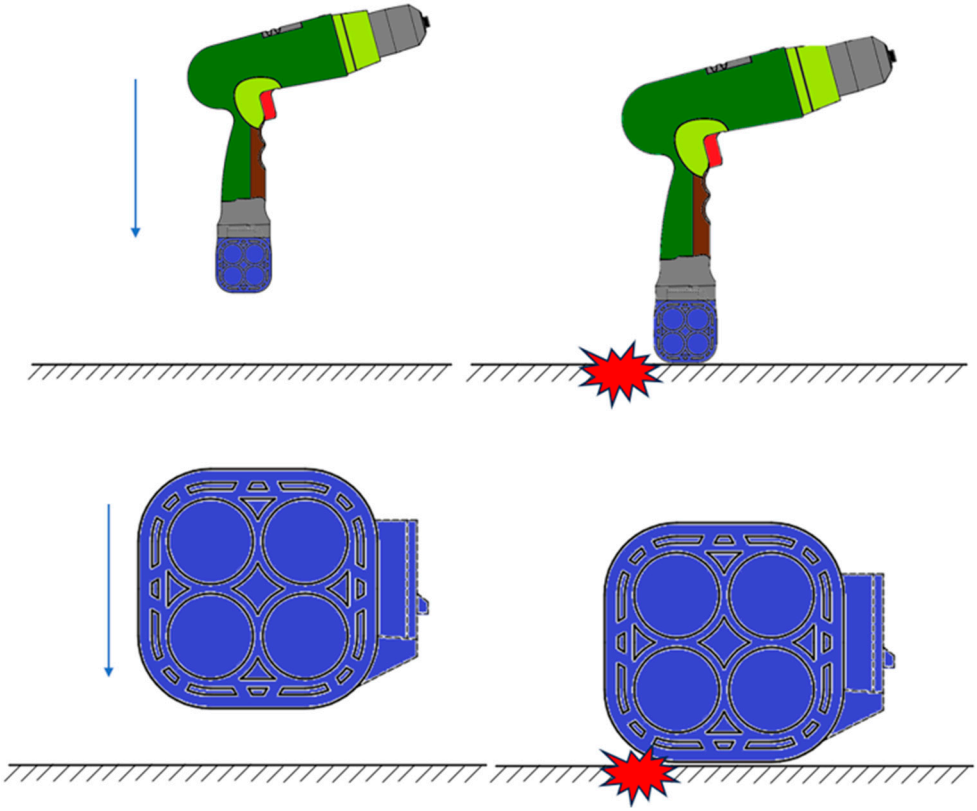

Figure 1. An example of a drop event with the whole electrical tool and separate battery.

The drop test is especially important because drops can occur frequently during the daily operation of batteries. Therefore, the electric tools industry recommends subjecting batteries to multiple-drop tests to ensure their durability and safety. The drop test can be performed with various configurations but involves several repetitions from various heights on the same side of the battery.

Today, in the industrial reality, there is a significant focus on reducing test failures. The traditional approach to postfailure component redesign is known as economically impractical. Consequently, there is a significant impetus towards the development of simulations capable of eliminating potential issues during testing.

Single-drop tests are popular because there are well-known methods for evaluating behavior during these tests, and there are many examples of such studies in the literature [14,15]. Unfortunately, single-drop tests are not enough to replace the need to simulate multiple-drop tests, which are not yet described in the scientific literature. This is because simulating only the highest drop does not consider the damage that builds up from previous drops. Therefore, creating an equivalent single-drop scenario for a multiple-drop

test is complex, mainly because single-drop calculations usually give results with fewer negative effects compared to real-world observations. Thus, there is a strong need to focus on simulating multiple-drop tests.

Optimization plays a critical role in many areas of engineering, aiming to make systems, structures, and technologies perform better, use less energy, and be more durable. It is widely used in areas such as aerospace [16], civil engineering [17], electronics [18], and the automotive industry [19,20]. The goal is always to find the most effective solutions that meet specific performance criteria under given constraints, which is particularly essential in high-stakes environments such as battery safety. The solution space includes many potential solutions, possibly hundreds or thousands. Therefore, it is not practical to explore each configuration in detail. This underscores the need to use optimization techniques to quickly find the best solution while reducing unnecessary computational costs. There are many well-known optimization methods documented in the literature, such as evolutionary algorithms, particle swarm optimization, artificial neural networks, and gradient methods [21]. These techniques find practical application in engineering tasks and are often integrated into commercial finite element method (FEM) software. In this particular example, we will evaluate the performance of a Quantum-Inspired Evolutionary Algorithm (QEA), a new approach that, so far, has not been practically implemented in the optimization of mechanical structures.

All the challenges mentioned above require solving several technical issues, including the automated running of multiple simulations, the smooth transfer of data from one analysis to the next drop test, the rebuilding of the geometry, the formulation of an optimization problem, and the determination of an optimal solution. In this research article, the authors aim to present their proposed solution to address these challenges using an automation algorithm and a QEA. This approach will be shown in a representative test scenario and an example of the geometry of the battery housing.

2. Materials and Methods

2.1. Optimization Algorithm

The Quantum-Inspired Evolutionary Algorithm (QEA), developed by Kuk-Hyun Han and Jong-Hwan Kim [22] approximately two decades ago, initially found application primarily in theoretical test functions, such as the knapsack problem. The QEA mimics some of the quantum mechanics phenomena [23–26]. The superposition state of information is typical for quantum mechanics and defines information granules as a qubit instead of bit found in the classical approach. The quantum bits, qubits, can exist in multiple states at once. The state of qubit can be represented using the Dirac bracket notation as follows:

$$|\psi\rangle = \alpha|0\rangle + \beta|1\rangle \quad (1)$$

where α and β are complex numbers that specify the probability of the corresponding states $|0\rangle$ and $|1\rangle$. The value $|\psi\rangle$ is determined in the moment of reading the information from the qubit—it means that the same weights α and β can lead to different resulting values of $|\psi\rangle$. The representation of all possible states of $|\psi\rangle$ can be visualized as a Bloch sphere (Figure 2). The QEA is based on such an approach; however, some simplifications are introduced; for example, the α and the β can be real numbers, and the Bloch sphere is reduced to a circle or part of the circle. The qubit value still depends on coefficients, and the results are known in the moment of reading the qubit value and, as a result, can be reduced to the classical bit value 0 or 1. The optimization algorithm presented in the paper operates on floating point number so that the group of qubits, after reading the values, the group of bits are converted to floating point numbers taking into account the box constraints of each design variable value and Gray code. The optimization program allows one to define the number of qubits that represent each design variable. The population of vectors of qubits is proceeded in each step of QEA like in typical evolutionary algorithms.

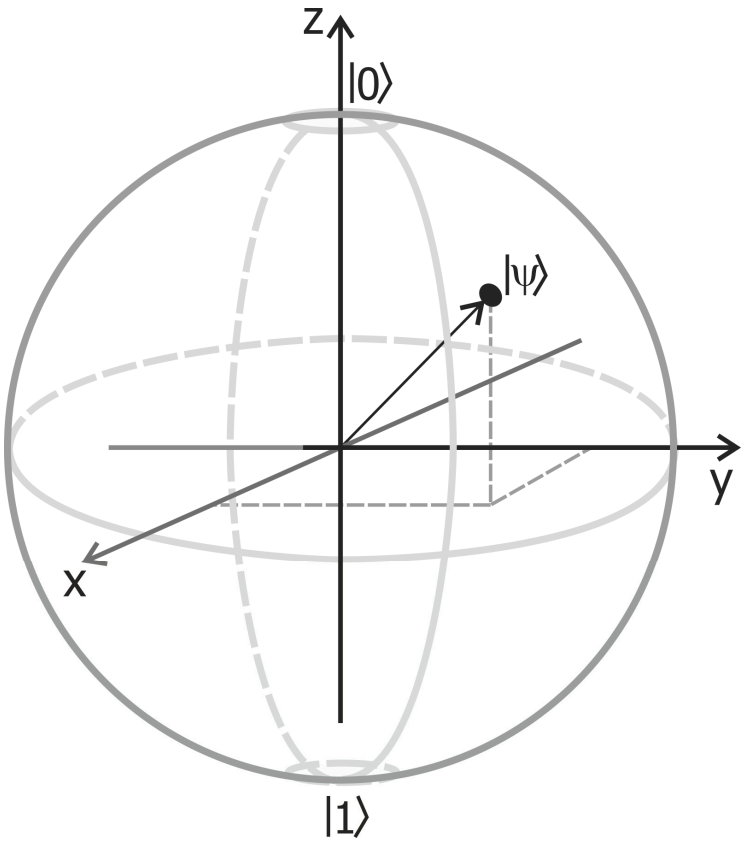

Figure 2. Bloch sphere.

The QEA operates on qubits and works similarly to evolutionary algorithms. Typical operators like crossover and mutation can be used to modify qubits but also are typical for QEA operators working like quantum gates. Quantum gates modify the α and β coefficients. The master direct problem and the slave optimization algorithm [27] approach is used to perform the computations. The flowchart of the QEA is shown in Figure 3. The starting population can be defined in a random way, but in the presented approach, the Hadamard gate is used for each qubit, and so the probability of 0 and 1 values during readout is the same. The parameters of all qubits and internal variables are stored, and the direct problem is solved for each individual (after reading the values of qubits and converting them to floating-point design variables values). The objective functions and previous state of qubits and variables are transferred to the QEA, and one step of selection and modification of qubits is performed. The selection in QEA leads to the modification of qubits with the influence of the best performing solution in the population. The objective function is obtained again for the modified population in case the end of computation condition is not fulfilled. The end-computation condition can be formulated as a desired best value of objective function, the number of iterations without objective function improvement, or maximum number of iterations.

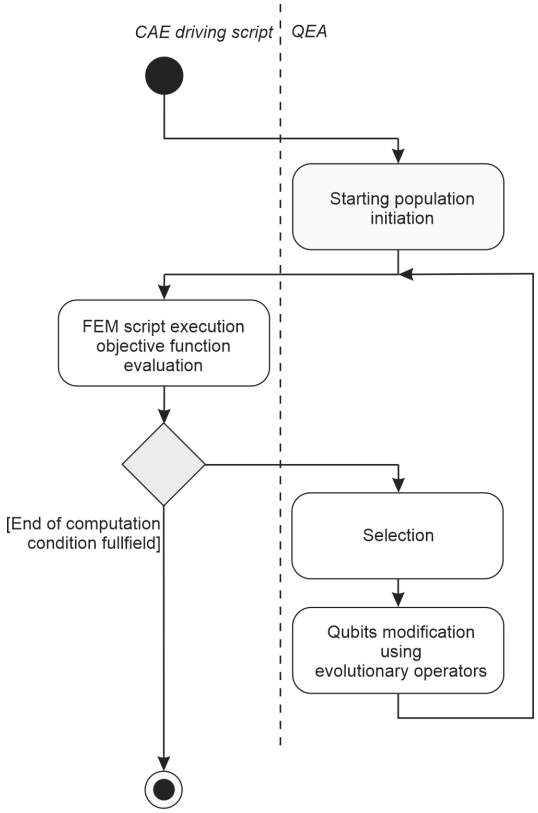

Figure 3. Flowchart of QEA.

2.2. Problem Formulation

The goal of this analysis is to achieve an optimal design that can effectively withstand the challenges posed by multiple-drop test scenarios. This involves fine-tuning various parameters to find the configuration in which the results are affected the least by damage after several drop tests. The objective function should be defined in a way that allows it to select the best individual from a design case, where in each configuration, there has been no damage; secondly, in all configurations, damage occurs; and thirdly, in one where both situations occur. Therefore, it was decided to use a sum of damage indicator and deformation. Mathematically, this problem can be described as minimizing the total amount of material removed when certain thresholds for damage indicators and plastic deformations are reached. The minimalization problem can be described by minimalization of objective function J_0:

$$\min_{P} J_0(\mathbf{P}) \tag{2}$$

where

$$J_0(\mathbf{P}) = a \cdot N(\mathbf{P}) + b \cdot \varepsilon_{p\_max}(\mathbf{P}) \tag{3}$$

where $N(\mathbf{P})$ is the quantity of deleted elements due to exceeding the failure criterion, $\varepsilon_{p\_max}(\mathbf{P})$ is the max equivalent plastic deformation from Misses theorem, and a, b are weight factors. $\mathbf{P}$ is the vector of design variables, which is represented by vector with the floating-point representation as follows:

$$\mathbf{P} = [P_1, P_2, \ldots, P_n] \tag{4}$$

where P_i—geometry parameter. Restrictions C on genes are imposed in the following way:

$$\mathrm{C} = \{\mathbf{P} : \forall \mathrm{i} \in \{1, \ldots, \mathrm{n}\} P_{imin} \leq P_i \leq P_{imax}\} \tag{5}$$

where P_{imin} is the design i minimal value, and P_{imax} is the design i maximal value.

2.3. Objective Function Evaluation

Objective function evaluation is performed based on FEM results (Abaqus 2023 software was used in the calculations). Explicit integration was used for the solution of dynamic problems, which is dedicated to this type of phenomenon with fast deformations close to the velocity of mechanical wave propagation in the material. The analysis of the housing is performed as a series of FEM problem solutions for drops of the same housing at various heights. The FEM software allows one to transfer the initial state (stress tensor, damage state), by choosing the previous analysis results, which are imported into the beginning of the next analysis step (next drop tests). For the automation of the entire process, the algorithm presented in Figure 4 was developed.

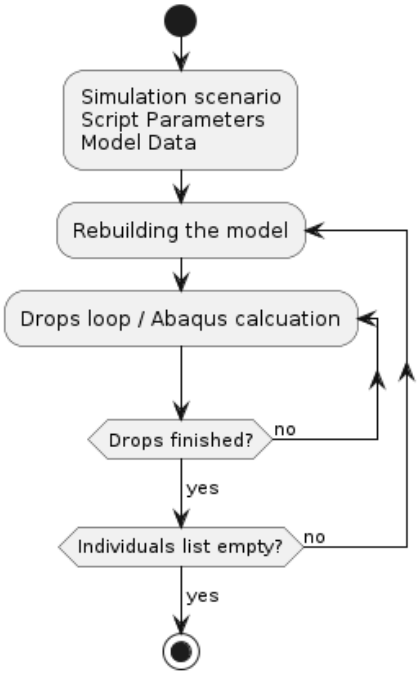

Figure 4. FEM analyses of drop tests of battery housing.

The input parameters can be categorized into three main sets. The first called model data relates to the simulation parameters, including geometry, material properties, discretization, contact mechanics, boundary conditions, required for performing a single drop test simulation. The geometry of the housing is modified according to the sets of design variables obtained from QEA.

The final set (script parameters) includes data related to the displacement value at which the analysis is to be terminated to prevent the excessive bouncing of the object. To prevent the phenomenon from occurring, e.g., when the analysis time is fixed, and the dropped object bounces higher than its initial position. The Abaqus solver has the capability to stop calculations if a certain threshold in the analysis is exceeded. In this case, it involves a filter that checks whether the characteristic points have exceeded the point from the beginning of the analysis.

For optimization purposes, the algorithm must possess the capability to modify the housing geometry. This functionality requires the integration of model construction within a loop. This involves the following parameter correction: models are reconstructed from scratch rather than modifying existing ones. This approach provides greater control over the model compared to modifying an existing one. Consequently, following the initial model reconstruction after parameter selection, a new model is constructed from the ground up, defining the complete analysis for the first drop.

This newly constructed model is included in the test loop, where velocities, directions, and repetitions are defined until the entire loop is completed. Within this loop, the following

conditions are evaluated. If it is the first drop for an individual within the loop, the initial state is deactivated. However, for further drops, this condition is activated, reading the initial state from the end of the previous analysis. Finally, the FEM solver calculations are executed. After the individual's computations have been finalized, the algorithm accesses the database of solutions and makes a systematic search through each finite element, recording the count of removed elements and the maximum value of plastic deformation, which are components of the above-mentioned objective function.

The objective function evaluation depends on damage evolution modeling in FEM. The constitutive model of plasticity used in this approach is well known as the Misses yield criterion, where equivalent stress $\overline{\sigma}_v, q$ are calculated, and σ_i are Cauchy stress tensor components:

$$q = \overline{\sigma}_v = \sqrt{\frac{1}{2}\left[(\sigma_1 + \sigma_2)^2 + (\sigma_2 + \sigma_3)^2 + (\sigma_3 + \sigma_1)^2\right]} \tag{6}$$

The second component connected to element deletion uses damage initiation and damage evolution criteria. For the equivalent plastic strain, damage initiation and damage evolution phenomenological model has to be evaluated.

The damage model in materials is divided by the initiation of damage at $D = 0$ and damage evolution what is presented in Figure 5. The damage parameter D is given as follows:

$$D(\varepsilon) = \int_{\varepsilon_p}^{\varepsilon_f} \frac{\mathrm{d}\varepsilon}{\overline{\varepsilon_f}(\eta, \overline{\Theta})} \tag{7}$$

where ε_p is the equivalent strain for damage initiation ($D = 0$), ε_f is equivalent strain for maximal damage ($D = 1$), and η is the stress triaxiality factor and $\overline{\Theta}$ Lode parameter. The stress triaxiality parameter is described as follows:

$$\eta = \frac{-p}{q} \tag{8}$$

where p depends on the mean stress of the following:

$$p = -\sigma_m = -\frac{1}{3}(\sigma_1 + \sigma_2 + \sigma_3) \tag{9}$$

q is the equivalent stress, and $\sigma_1, \sigma_2, \sigma_3$ are principal stress values.

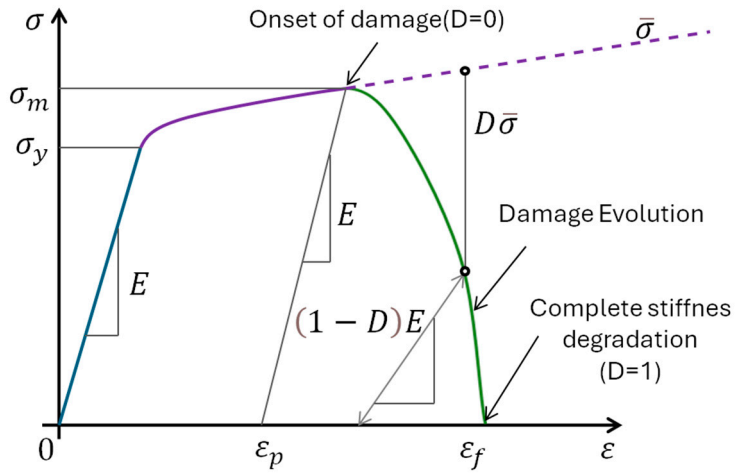

Figure 5. Uniaxial stress–strain curve.

After damage initiation ($D = 0$), stress σ in every single increment of analysis can be described as the scalar equation of damage with undamped (without damage) stress $\overline{\sigma}$ as follows:

$$\sigma = (1 - D)\overline{\sigma} \tag{10}$$

Element removal occurs when the material achieves maximum stiffness degradation. The degradation of elasticity, where the parameter is Young's modulus E, degrades to E' according to the following equation until it completely loses stiffness when $D = 1$, as shown below:

$$E' = (1 - D)E \tag{11}$$

Both conditions are critical points from the perspective of drop simulation. Without damage evolution (instead of simple element deletion at $D = 0$), the elements could collapse each by each in the area of contact with the floor, due to instantaneous exceeding strain deformation at failure in a contact area, additionally this kind of sudden removing of elements causes unnatural fluctuations of stiffness of the structure. Without taking into account stress states like the Lode parameter and stress triaxiality, the material could collapse too early, e.g., in a compression state, when in real materials, they demonstrate different behaviors during compression and tension.

3. Numerical Example

For the purposes of this study, a conceptual battery design is considered potentially suitable for use in a power tool. The design enables the construction of a cell pack in various configurations, depending on the power demand and battery capacity, which is shown in Figure 6.

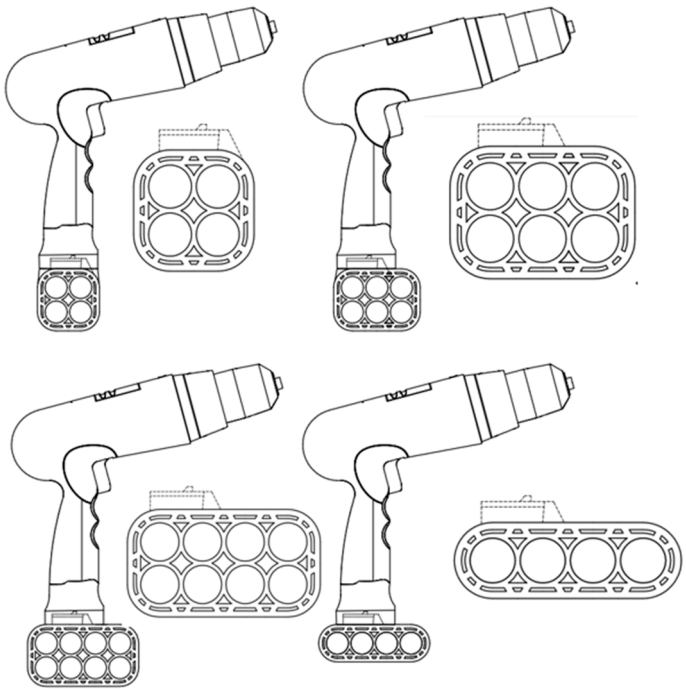

Figure 6. Battery configuration possibilities.

The main component of the housing, the corepack, holds the cells and facilitates the connection to the power tool. Additional protection is provided by welding covers on the front surfaces. The drawing excludes electronic components such as busbars and cables (Figure 7). This study, being experimental, focuses on optimizing the corepack.

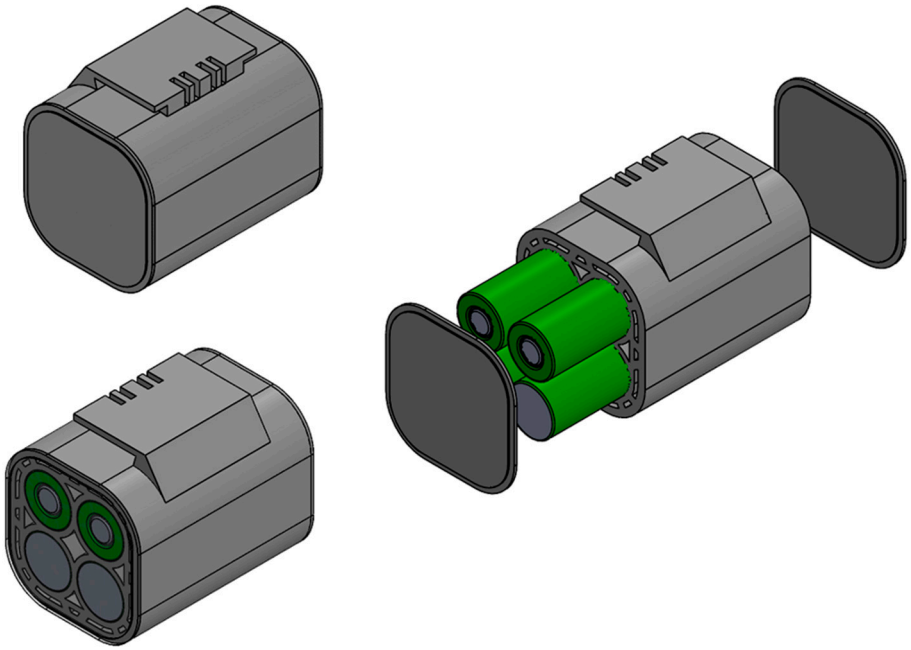

Figure 7. Conceptual project of battery (smallest configuration) which can be implemented in power tool.

Thus, the chosen optimization object is the smallest configuration core from which unnecessary structural elements have been removed to expedite the time-consuming calculations, as shown in Figure 8. This geometry is characterized by three fundamental design elements. The external part of the shape is called the damper (brown), and through the ribs (green), it is connected to the core (blue).

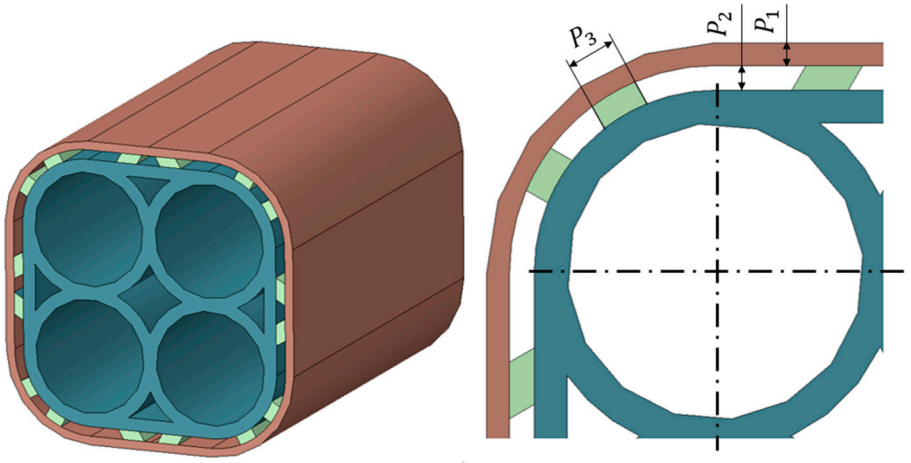

Figure 8. Geometry of the battery housing and design variables.

Point masses with weight of 0.07 kg represent cells and are connected by multipoint constraints with all six degrees of freedom on inner cylindrical surfaces of the housing as shown in Figure 9. The model was discretized using an eight-node linear brick element with reduced integration and hourglass control. The default mesh size was set to 0.4 mm and depending on parameters there are about 64,000 elements.

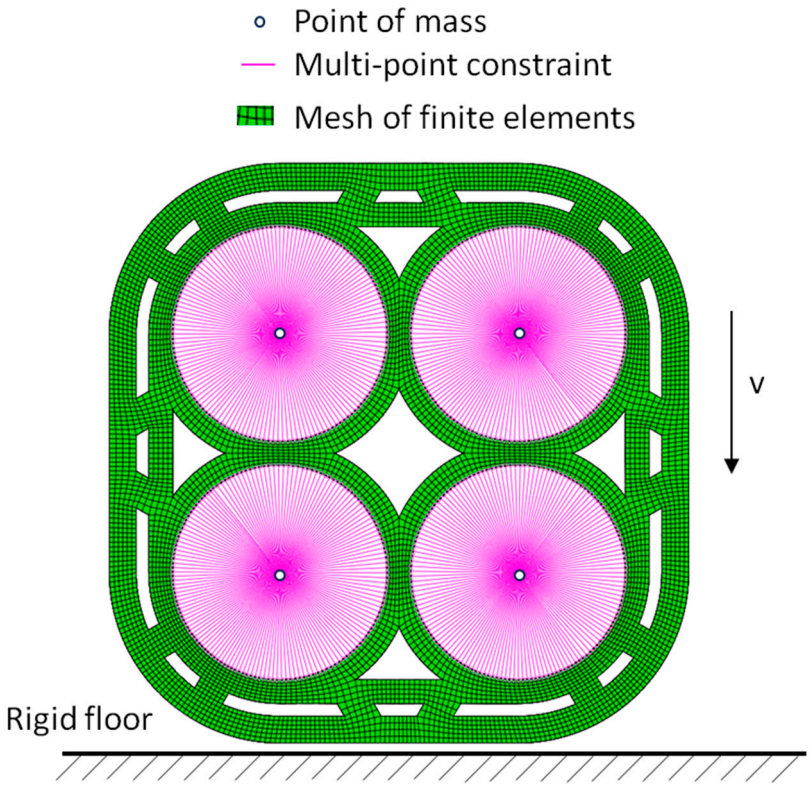

Figure 9. Discretization of the model and boundary conditions.

This geometric configuration is parameterized, and we will seek the optimal point within this design space. The constraints on the design parameters are as follows:

$$\mathbf{P} = \{P_1, P_2, P_3 \mid P_1 \in (1\,\text{mm}, 3\,\text{mm}),\ P_2 \in (1\,\text{mm}, 3\,\text{mm}),\ P_3 \in (1\,\text{mm}, 3\,\text{mm})\} \quad (12)$$

The model assumes an elastic–plastic material model, with damage initiation and damage evolution criterion dependent of stress triaxiality. Simplified in a homogenized form the PA6-GF30 short fiber reinforcement material was described with density = 1350 $\frac{\text{kg}}{\text{m}^3}$, Young Modulus = 9.1 GPa, and Poisson's ratio = 0.34. The damage initiation criterion was presented with the following configuration, with linear damage evolution set at 0.1 mm. Fracture locus is defined in the Table 1.

Table 1. Parameters of the damage initiation material.

Fracture Strain [mm/mm]	Stress Triaxiality Factor
1.014	−0.33
0.014	0
0.014	0.33

True plastic stress strain is defined in the following table (Table 2).

Table 2. Plasticity parameters.

Yield Stress [MPa]	Plastic Strain [mm/mm]
99	0
175	0.01459

The test scenario involves two drops in the same direction from two different heights, corresponding to free-fall velocities v (10.3 $\frac{\mathrm{m}}{\mathrm{s}}$ and 16.5 $\frac{\mathrm{m}}{\mathrm{s}}$) which was calculated from the transformation of free-fall equation as follows:

$$v = \sqrt{2gh} \tag{13}$$

where g is the gravity acceleration, and h is the height of the freefall drop.

It is essential to emphasize that any deterministic scenario can be implemented in this analysis, including multiple repetitions, various directions, and varying heights.

The parameters (QEA) are as follows: number of individuals—30; number of qubits per design variable—6. Changes in the objective function value and design variables for chosen optimization problems are shown in Figure 10.

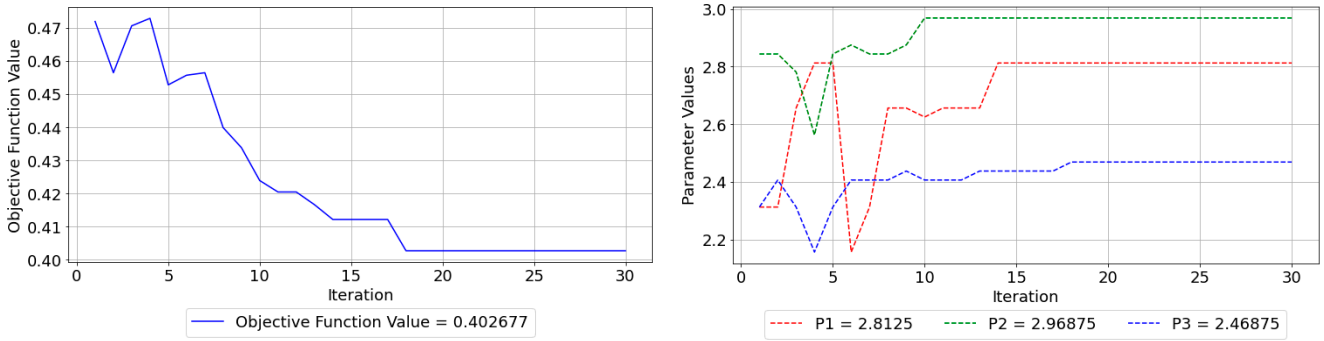

(**a**) (**b**)

Figure 10. (**a**) Objective function in function of iteration number; (**b**) design variables values in function of iteration number.

The points visited in design space during optimization are shown in Figure 11. The filtered graph shows solutions with an objective function value below 0.5.

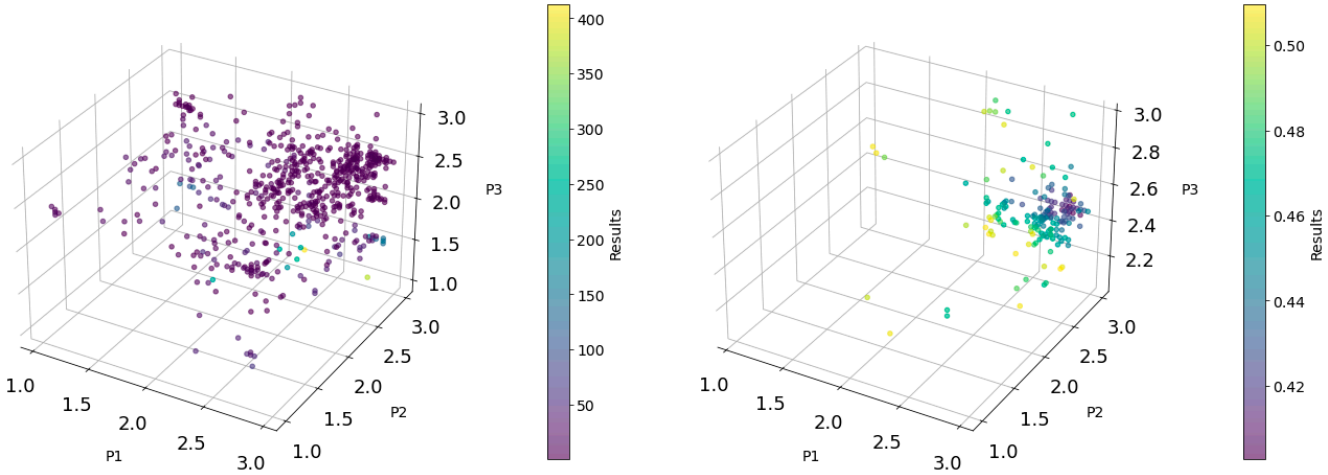

(**a**) (**b**)

Figure 11. Charts of the distribution of the objective function in design space during QEA optimization with (**a**) all points analyzed points in design space and (**b**) filtered points for the objective function below 0.5.

A representative sample with parameters $P_1 = 2.89553$, $P_2 = 2.99335$, $P_3 = 1.25013$, which sustained significant damage, is depicted in Figure 12 on the map of equivalent plastic strain after the second drop. One can observe the rupture of the ribs and the propagation of the cracks. In this case, 591 finite elements were removed.

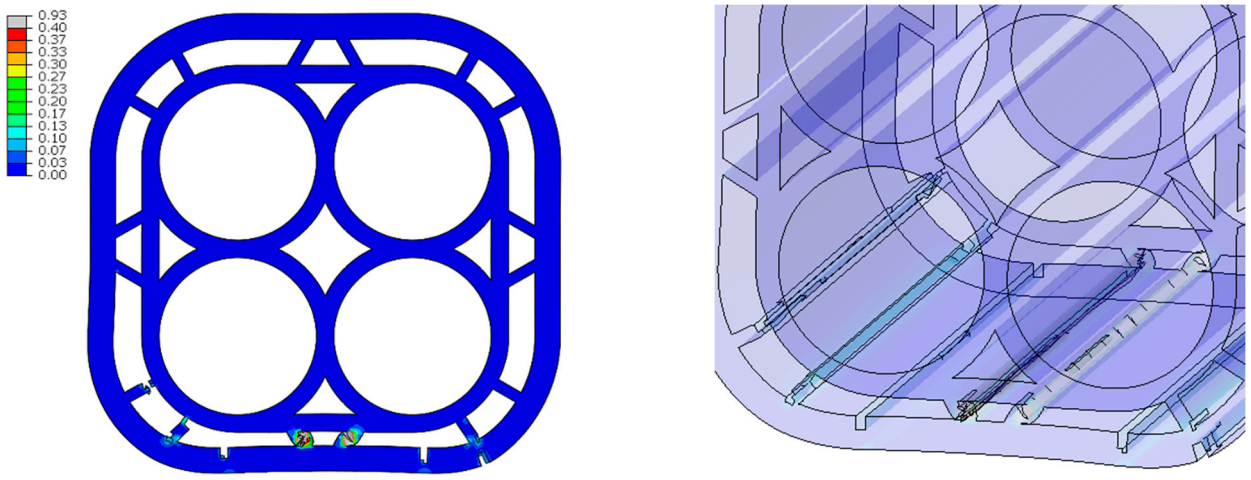

(**a**) (**b**)

Figure 12. Map of equivalent plastic strain for damaged example: (**a**) general overview and (**b**) transparent 3D detailed view.

The map of the equivalent plastic equivalent strain after first and second drop for the best-found solution is shown in Figure 13.

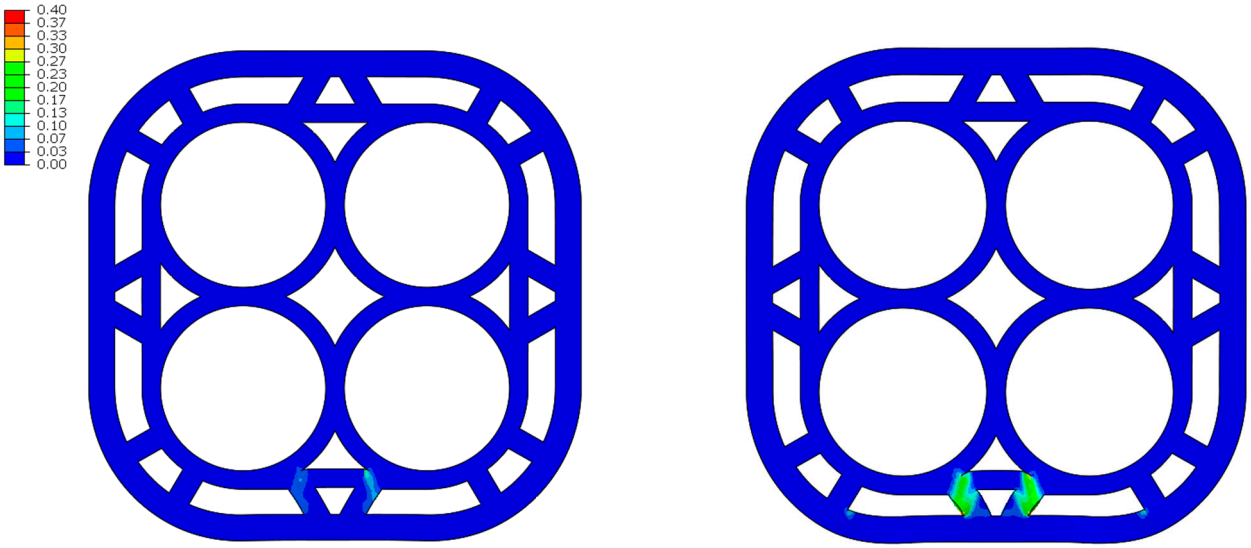

(**a**) (**b**)

Figure 13. Map of equivalent plastic strains for optimized structure (**a**) at the end of the first drop and (**b**) at the end of the second drop.

4. Conclusions

This study highlights the effectiveness of the Quantum-Inspired Evolutionary Algorithm (QEA) in optimizing the structural design of lithium-ion battery housings subjected to multiple-drop tests. This research has successfully demonstrated how the QEA can be used to meet the specific needs of battery safety improvements, presenting its potential to significantly reduce damage from mechanical impacts, which are common in everyday use scenarios.

The authors findings show that the QEA not only identifies robust designs that withstand multiple impacts but also optimizes the design parameters to increase the safety and durability of lithium-ion batteries.

Moreover, the integration of QEA with the finite element method (FEM) simulations presents a significant advancement in battery housing design. This combined approach allows for a better understanding of how different design modifications affect the structural integrity of battery housings under real-world impact conditions.

Additionally, this research introduces an automated algorithm developed to let integration of QEA with FEM simulations for battery housing designs. The automation algorithm significantly improves the iterative design evaluation process by automatically setting up, running and analyzing the results of multiple drop tests. This automation is crucial in fast cycling through design iterations, allowing engineers to quickly converge on optimal solutions without the manual work traditionally associated with such comprehensive simulations.

The algorithm not only applies QEA for initial design optimization but also manages the data flow between successive drop tests, ensuring that the results from one test inform the setup of the next. This continuity is vital for accurately simulating the cumulative damage from multiple impacts, a scenario that closely mimics real-world use of batteries. By maintaining a dynamic link between simulation phases, the automated system effectively captures the progressive nature of damage under repeated mechanical stress, which is often overlooked in less advanced testing methodologies.

These advanced computational tools allow us to design battery housings that are much more resistant to damage from drops and impacts, which are common during everyday use. By ensuring that battery housings can withstand such stresses, we significantly reduce the risk of battery failure, including dangerous scenarios such as thermal runaway. This not only extends the life of the batteries but also ensures that they operate safely under various conditions, providing a significant benefit in terms of consumer safety and product reliability.

Author Contributions: Conceptualization, W.K. and A.R.; methodology, W.K. and A.R.; software, W.K. and A.R.; writing—original draft preparation, A.R.; writing—review and editing, W.K. and A.R. All authors have read and agreed to the published version of the manuscript.

Funding: The research was co-financed under grant no. DWD/6/0475/2022 is supported by the Ministry of Science and Higher Education in Poland and a research subsidy from the Faculty of Mechanical Engineering, Silesian University of Technology, 2024.

Data Availability Statement: The data presented in this study are available upon request from the corresponding author.

Conflicts of Interest: The authors declare that they have no conflicts of interest.

References

1. Weydanz, W. APPLICATIONS—PORTABLE | Power Tools: Batteries. In *Encyclopedia of Electrochemical Power Sources*; Elsevier: Amsterdam, The Netherlands, 2009; pp. 46–52. [CrossRef]
2. Blomgren, G.E. The Development and Future of Lithium Ion Batteries. *J. Electrochem. Soc.* **2017**, *164*, A5019–A5025. [CrossRef]
3. Diouf, B.; Pode, R. Potential of lithium-ion batteries in renewable energy. *Renew. Energy* **2015**, *76*, 375–380. [CrossRef]
4. Abada, S.; Marlair, G.; Lecocq, A.; Petit, M.; Sauvant-Moynot, V.; Huet, F. Safety focused modeling of lithium-ion batteries: A review. *J. Power Sources* **2016**, *306*, 178–192. [CrossRef]
5. Feng, X.; Ren, D.; He, X.; Ouyang, M. Mitigating Thermal Runaway of Lithium-Ion Batteries. *Joule* **2020**, *4*, 743–770. [CrossRef]
6. Cheng, K.W.E.; Divakar, B.P.; Wu, H.; Ding, K.; Ho, H.F. Battery-Management System (BMS) and SOC Development for Electrical Vehicles. *IEEE Trans. Veh. Technol.* **2011**, *60*, 76–88. [CrossRef]
7. Wang, Q.; Ping, P.; Zhao, X.; Chu, G.; Sun, J.; Chen, C. Thermal runaway caused fire and explosion of lithium ion battery. *J. Power Sources* **2012**, *208*, 210–224. [CrossRef]
8. Wen, J.; Yu, Y.; Chen, C. A Review on Lithium-Ion Batteries Safety Issues: Existing Problems and Possible Solutions. *Mater. Express* **2012**, *2*, 197–212. [CrossRef]
9. Lai, X.; Yao, J.; Jin, C.; Feng, X.; Wang, H.; Xu, C.; Zheng, Y. A Review of Lithium-Ion Battery Failure Hazards: Test Standards, Accident Analysis, and Safety Suggestions. *Batteries* **2022**, *8*, 248. [CrossRef]
10. Chen, Y.; Kang, Y.; Zhao, Y.; Wang, L.; Liu, J.; Li, Y.; Liang, Z.; He, X.; Li, X.; Tavajohi, N.; et al. A review of lithium-ion battery safety concerns: The issues, strategies, and testing standards. *J. Energy Chem.* **2021**, *59*, 83–99. [CrossRef]

11. *ISO 16750-3*; Road Vehicles—Environmental Conditions and Testing for Electrical and Electronic Equipment—Part 3: Mechanical Loads. International Organization for Standardization: London, UK, 2012.
12. Economic Commission for Europe of the United Nations (UNECE). *Uniform Provisions Concerning the Approval of Vehicles with Regard to Specific Requirements for the Electric Power Train*; UN Regulation No. 100, Revision 3; UNECE: Geneva, Switzerland, 2013.
13. International Electrotechnical Commission. *Secondary Cells and Batteries Containing Alkaline or Other Non-Acid Electrolytes—Safety Requirements for Portable Sealed Secondary Cells, and for Batteries Made from Them, for Use in Portable Applications—Part 2: Lithium Systems*; IEC 62133-2; IEC: London, UK, 2017.
14. Shu, D.W.; Shi, B.J.; Luo, J. Shock Simulation of Drop Test of Hard Disk Drives. In *Structural Dynamics of Electronic and Photonic Systems*; Suhir, E., Steinberg, D.S., Yu, T.X., Eds.; Wiley: Hoboken, NJ, USA, 2011; pp. 337–356.
15. Yeh, M.-K.; Huang, T.-H. Drop Test and Finite Element Analysis of Test Board. *Procedia Eng.* **2014**, *79*, 238–243. [CrossRef]
16. Keane, A.J.; Scanlan, J.P. Design search and optimization in aerospace engineering. *Phil. Trans. R. Soc. A* **2007**, *365*, 2501–2529. [CrossRef] [PubMed]
17. Rajput, S.P.S.; Datta, S. A review on optimization techniques used in civil engineering material and structure design. *Mater. Today Proc.* **2020**, *26*, 1482–1491. [CrossRef]
18. Wang, Y.Y.; Lu, C.; Li, J.; Tan, X.M.; Tse, Y.C. Simulation of drop/impact reliability for electronic devices. *Finite Elem. Anal. Des.* **2005**, *41*, 667–680. [CrossRef]
19. Christensen, J.; Bastien, C. *Nonlinear Optimization of Vehicle Safety Structures: Modeling of Structures Subjected to Large Deformations*; Elsevier: Amsterdam, The Netherlands, 2016.
20. Sebastjan, P.; Kuś, W. Optimization of material distribution for forged automotive components using hybrid optimization techniques. *Comput. Methods Mater. Sci.* **2021**, *21*, 63–74. [CrossRef]
21. Burczyński, T.; Kuś, W.; Beluch, W.; Długosz, A.; Poteralski, A.; Szczepanik, M. *Intelligent Computing in Optimal Design*; Solid Mechanics and Its Applications; Springer International Publishing: Cham, Switzerland, 2020.
22. Han, K.-H.; Kim, J.-H. Quantum-inspired evolutionary algorithm for a class of combinatorial optimization. *IEEE Trans. Evol. Computat.* **2002**, *6*, 580–593. [CrossRef]
23. Kuś, W.; Mrozek, A. Quantum-inspired evolutionary optimization of SLMoS2 two-phase structures. *Comput. Methods Mater. Sci.* **2022**, *22*, 67–78. [CrossRef]
24. Zhang, G. Quantum-inspired evolutionary algorithms: A survey and empirical study. *J. Heuristics* **2011**, *17*, 303–351. [CrossRef]
25. Lahoz-Beltra, R. Quantum Genetic Algorithms for Computer Scientists. *Computers* **2016**, *5*, 24. [CrossRef]
26. Da Silveira, L.R.; Tanscheit, R.; Vellasco, M.M.B.R. Quantum inspired evolutionary algorithm for ordering problems. *Expert Syst. Appl.* **2017**, *67*, 71–83. [CrossRef]
27. Burczyński, T.; Pietrzyk, M.; Kuś, W.; Madej, Ł.; Mrozek, A.; Rauch, Ł. *Multiscale Modelling and Optimisation of Materials and Structures*; Wiley: Hoboken, NJ, USA, 2022.